Supporting Information

for

Engineering multifunctional metal/protein hybrid nanomaterials as tools for therapeutic intervention and high-sensitivity detection

Antonio Aires,[‡a] David Maestro,[‡b] Jorge Ruiz del Rio,[b] Ana R. Palanca,[b,c] Elena Lopez-Martinez,[a] Irantzu Llarena,[a] Kalotina Geraki,[d] Carlos Sanchez-Cano,*[a] Ana V. Villar,*[be] and Aitziber L. Cortajarena*[af]

[a] Center for Cooperative Research in Biomaterials (CIC biomaGUNE), Basque Research and Technology Alliance (BRTA). Paseo de Miramón 194, 20014, Donostia-San Sebastián, Spain.

[b] Instituto de Biomedicina y Biotecnología de Cantabria (IBBTEC), CSIC-Universidad de Cantabria, Albert Einstein 22, 39011, Santander, Spain.

[c] Departamento de Anatomía y Biología Celular, Universidad de Cantabria, Avd. Herrera Oria s/n, 39011, Santander, Spain.

[d] Diamond Light Source, Harwell Science and Innovation Campus, RG20 6RE, England.

[e] Departamento de Fisiología y Farmacología, Universidad de Cantabria, Avd. Herrera Oria s/n, 39011, Santander, Spain.

[f] Ikerbasque, Basque Foundation for Science, Mª Díaz de Haro 3, 48013 Bilbao, Spain.

* To whom correspondence should be addressed: alcortajarena@cicbiomagune.es , csanchez@cicbiomagune.es, and anavictoria.villar@unican.es

‡ These authors contributed equally to this work.

Table of Contents

Materials and Methods

Materials

All chemical reagents were purchased from Sigma-Aldrich. All solutions were prepared from Milli-Q water (Milli-Q Ultrapure water systems, Millipore).

Protein Design, Cloning and Molecular Biology

Consensus tetratricopeptide repeat (CTPR) proteins were created and characterized as previously described.[1, 2] CTPR390 **[1]** was created and characterized as previously described.[3] The CTPR proteins present an extra sequence at the N-terminal end due to the cloning strategy (GAMGS), and an additional helix at the C-terminal end for improved solubility (AEAKQNLGNAKQKQG). CTPR2-C2_4Cys ($C2_{NC}$) module **[2]** (AEAWCNLGCAYYKQGDYDEAIEYYQKALELDPRSACAWYCLGNAYYKQGD YDEAI EYYQKALELDPRS) was created as previously described.[3] By combinations of the modules **1**, $C2_{NC}$ and W, two proteins were generated, CTPR4-W-C2_4Cys-W **[3]** and CTPR5-C2_4Cys-CTPR390 **[4]**. For this purpose, DNA encoding the CTPR2-C2_4Cys, W, and CTPR390 modules were fused using a modular cloning strategy based on Hind III, Bam HI, and Bgl II digestion.[4] The genes encoding the two proteins were generated, **[3]** and **[4]** were cloned into the pProEx-HTA vector and their identities verified by DNA sequencing (Stab Vida).

Protein Expression and Purification

Overnight cultures of C41 (DE3) cells harboring the genes for the desired protein in pProEx-HTA vector, coding for N-terminal His6-tag and ampicillin resistance were diluted by 1:100 in LB medium with 0.1 mg/ml ampicillin. Cells were grown at 37ºC with agitation of 220 rpm until optical density reached 0.6-0.8. Protein expression was induced with 1 mM isopropyl β-d-thiogalactoside (IPTG) .The bacteria were further incubated for 16 hour at 20ºC and then harvested by centrifugation 15 min at 4500 rpm. The cell pellets were resuspended in 50 mM Tris, 500 mM NaCl, pH 8.0 and lysed by sonication. The lysates were centrifuged for 45 min at 10000 rpm, and proteins were purified from the supernatant using 5 mL HisTrap Q column (GE Healthcare). The proteins were eluted with 50 mM Tris, 500 mM NaCl, 300 mM imidazole, pH 8.0. Then eluted CTPR proteins were further subjected to Tobacco Etch Virus (TEV) protease cleavage for 16 hours at 20ºC to remove the His6-tag and further purified by fast protein liquid chromatography

(FPLC) using a HiLoad 16/60 Superdex 200 column equilibrated with 50 mM Tris, 500 mM NaCl, 300 mM imidazole, pH 8.0. Protein concentration was measured by UV absorbance at 280 nm, using extinction coefficients at 280 nm calculated from amino acid composition.

Synthesis of protein-stabilized gold nanoclusters

The protein-stabilized AuNC were synthesized using a modified protocol based on a previously reported procedure.[5] Briefly, 1000 µL of protein at 20 µM were mixed with $HAuCl_4$ (60 µL 10 mM, 30 eq. respect to protein) for 1 hour at 20ºC. Then, the reduction of the gold ions was achieved by adding 60 µL of sodium ascorbate at 1M (100 eq. respect to gold ions). The reaction was incubated at 50°C for 72 h. The protein-stabilized AuNC were purified via gel filtration using a Sephadex G-25M column and then stored at 4°C. The absorption and fluorescence spectra of protein-stabilized AuNC were measured using a Synergy H1 microplate reader.

Circular Dichroism (CD)

The protein secondary structure was examined by CD using a Jasco J-815 spectrometer (JASCO Corporation, Tokyo, Japan). CD spectra of the protein alone and the protein-stabilized AuNC were acquired at 10 µM protein concentration in a 1 mm path length cell at 25ºC using a 1 nm bandwidth with 1 nm increments and 10 s average time.

Steady-state optical spectroscopy

UV-visible absorption spectra were measured in a Jasco V-630 Bio spectrophotometer. Fluorescence spectra were recorded in a LS-55 PerkinElmer spectrofluorometer with a slit of 1 nm band-pass. All the absorption and emission measurements were performed using a standard quartz cuvette of 1 cm path length. The fluorescence quantum yield (Φ_x) was calculated using anthracene in ethanol as a reference (Φ_{ref} = 0.27, λ_{exc} = 370 nm and λ_{em} = 423 nm) and the following formula:

$$\phi_x = \phi_{ref} \ \frac{Grad_x}{Grad_{ref}} \left(\frac{\eta_x^2}{\eta_{ref}^2} \right)$$

where $Grad_x$ and $Grad_{ref}$ are the gradient from the plot of integrated fluorescence intensity versus absorbance at excitation wavelength, for the sample and the reference,

respectively, and η_x and η_{ref} are the refractive indexes of the solvents, PBS (150 mM NaCl, 50 mM phosphate pH 7.4), and ethanol, respectively.

Time–resolved fluorescence spectroscopy

Fluorescence lifetime measurements were carried out exciting with a 370 nm PDL 828 Picoquant Sepia laser, with a 50 ps pulse duration. The fluorescence was dispersed by a spectrometer (SP2500, Acton Research), and detected with a Picoquant PMA Hybrid-Photomultiplier Assembly with a transit time spread of less than 50 ps and a Picoquant Hydraharp time-correlated single photon counting (TCSPC) electronics. The resulting time resolution after de-convolution of the instrumental response function was better than 50 ps. Measurements were carried out in solutions placed in 2 mm-optical path quartz cuvettes.

Matrix assisted laser desorption ionization (MALDI) mass spectrometry

Mass spectra were acquired on an Applied Biosystems Voyager Elite MALDI-TOF mass spectrometer with delayed extraction (Applied Biosystems, Framingham, MA, USA) equipped with a pulsed N_2 laser (λ= 337 nm). Sinapic acid was used as matrix. An extraction voltage of 20 kV was used. All mass spectra were acquired in positive reflection mode using delayed extraction with an average of 50−100 laser shots. MALDI-TOF sample preparation included 1 μL of the sample mixed with 3 μL of sinapic acid in 50:50 water/acetonitrile with 0.01% TFA. Then, 1 μL of the mixture was deposited onto the MALDI plate and allowed to air-dry. The instrument was externally calibrated using monoisotopic peaks from the sinapic acid matrix (MH^+ at m/z 225.071).

Inductively coupled plasma mass spectrometry (ICP-MS)

100 μL approximately at 100μM of each FPLC purified metal NC were mixed with 300 μL of 37% HCl and the resultant suspension was sonicated for 30 minutes at 40ºC. Finally, 2700 mL of bi-distilled water was added. The Au concentration was determined by measuring the sample using an iCAP-Q ICP-MS (Thermo Scientific, Bremen, Germany) equipped with an autosampler ASX-520 (Cetac Technologies Inc., NE, USA) (n=3) and QtegraTM v2.6 (Themo Scientific).

Stability of the protein-stabilized AuNC

The storage stability of the protein stabilized AuNC in physiological conditions was evaluated during one month at 4ºC by fluorescent spectrophotometry using a Varioskan microplate reader (Thermo Scientific). The stability under physiological conditions (PBS and human plasma (HP)) was examined during one week at 37ºC by fluorescent spectrophotometry using a Varioskan microplate reader (Thermo Scientific).

Transmission Electron Microscopy (TEM)

Ultrathin carbon films on holey carbon support film, 400 mesh copper grids (TED PELLA INC.) were exposed to glow-discharge treatment before sample deposition. TEM samples were prepared by depositing 5 μL of the sample solution on the grid. After 3 min, the excess solution was removed from the grid using filter paper. To remove the deposited salt, the grid was then washed with a drop of water, and the excess water was dried using filter paper. Micrographs were recorded using a JEOL JEM 2100F electron microscope operating at 200 kV with a Field Emission Gun. HAADF STEM images were acquired on a JEOL JEM-2100F UHR microscope at 200 kV in scanning mode, with a probe size of 1.5 nm and a choice of the camera length that ensures an inner detector angle of 75 mrad (HAADF) to enhance the contrasts of the metal atoms on the carbon support film.

X-ray photoelectron spectroscopy (XPS)

X-ray photoelectron spectroscopy measurements were performed with a SPECS SAGE HR 100 spectrometer equipped with a 100 mm mean radius PHOIBOS analyzer and a nonmonochromatic X-ray source (Mg Kα line of 1253.6 eV energy and 250 W), placed perpendicular to the analyzer axis and calibrated using the 3d5/2 line of Ag, with a full width at half maximum of 1.1 eV. All measurements were made in an ultrahigh vacuum chamber at a pressure of around 8×10^{-8} mbar. An electron flood gun was used to neutralize for charging. Measurements were conducted directly on dry deposited films, which were previously washed with absolute ethanol and cut into samples of 1 cm × 1 cm. The analysis of spectra was done with CasaXPS 2.3.15dev87 software.

Binding Properties of 4-AuNC

The ligand binding capability of the CTPR protein scaffold upon the generation of AuNC was studied using the CTPR390 protein (**1**) and its target peptide. CTPR390 was designed

to bind the C-terminal sequence of Hsp90 protein.[3] CTPR5-C2_4Cys-CTPR390 **[4]** and CTPR5-C2_4Cys-CTPR390-AuNC (**4-AuNC**) binding affinity to Hsp90 peptide was determined by fluorescence anisotropy titrating with increasing amounts of **4** and **4-AuNC** into a 50 nM fluorescein-labeled Hsp90 peptide solution.[6, 7] Fluorescence intensities were recorded in a LS-55 PerkinElmer spectrofluorometer equipped with excitation and emission polarizers. Excitation was accomplished with a 5 nm slitwidth at 492 nm and the emission recorded at 516 nm with slit widths of 5 nm.

Cell culture and AuNC incubation

NIH-3T3 fibroblast cell line was purchased from American Type Culture Collections (Manassas, VA, USA). This cell line was grown as monolayer in Dulbecco's Modified Eagle's Medium (DMEM) supplemented with fetal bovine serum (FBS) at a final concentration of 10%, 2 mM L-glutamine, 0.25 μg mL-1 fungizone and 100 Units of penicillin and 100μg mL-1 streptomycin. All the media, serum, L-glutamine, fungizone, and antibiotics were purchased from GIBCO. Cell lines were maintained at 37°C in a humidified atmosphere consisting of 75% air and 5% CO_2 in an incubator. 500 μL of **4-AuNC** dispersed in PBS were diluted in medium containing 10% FBS at the desired concentration. The resulting sample was filtered through a 0.22 μm Millex-GP filter (Merck-Millipore Darmstadt, Germany). Cells were incubated with protein stabilized AuNC for 24 h. Then, cell media with **4-AuNC** was removed and cells were washed with phosphate buffered saline (PBS) for complete removal of protein stabilized AuNC from cell medium. Then fresh cell media was added to continue further viability studies.

Enzymatically (collagenase 0.7 mg/ml, trypsin 1.4 mg/ml and DNase 150 μg/ml) isolated adult cardiac fibroblasts from mice (C57BL6 strain) were centrifuged, filtrated and maintained in DMEM containing 10% FBS, 10% DBS and 100 U/ml penicillin-streptomycin at 37 °C in 5% CO2. At 80% confluence, cells were treated with recombinant TGFβ1 (0.3 ng/ml) (R&D Systems) and **4-AuNC** (0.2, 0.4, 0.8, 1.5, or 3 μM) for 24 h. Then, cell media with **4-AuNC** was removed and cells were washed with phosphate buffered saline (PBS) for complete removal of protein stabilized AuNC from cell medium. Then fresh cell media was added to continue further viability studies. Results included triplicate of three independent assays of low passage cells (p2).

In vitro cytotoxicity assay

Resazurin dye (Sigma-Aldrich) was used as indicator of cell viability in the proliferation and cytotoxicity assays. To assess cell viability, NIH-3T3 fibroblast cells and isolated adult cardiac fibroblasts from mice (C57BL6 strain), at 80% of confluence were treated with recombinant TGFβ1 (0.3 ng/ml) (R&D Systems) and **4-AuNC** at different concentrations for 24 h. Then, cell media with **4-AuNC** was removed, cells were washed with phosphate buffered saline (PBS) for complete removal of protein stabilized AuNC from cell medium, fresh cell media was added to the cells and incubated at 37°C and 5% CO_2. After 5 days, the medium was replaced with fresh media containing 10% of resazurin dye (1mg/mL PBS). Cells were maintained in the incubator at 37°C and 5% CO2 for 3 hours and then, a Varioskan microplate reader (Thermo Scientific) was used to determine the amount of resazurin reduced by measuring the absorbance of the reaction mixture (λ_{exc}=570 nm, λ_{em}=600 nm). 500 µl of 10% of resazurin dye was added to empty wells as a negative control. The viability of the cells was expressed as the percentage of absorption of treated cells in comparison with control cells (without AuNC). All experiments were carried out in triplicate.

In vitro 4-AuNC internalization

Inductively coupled plasma mass spectrometry. Adult cardiac fibroblasts from mice (C57BL6 strain) were maintained in DMEM containing 10% FBS, 10% DBS and 100 U/ml penicillin-streptomycin at 37 °C in 5% CO_2. Around $5x10^5$ cells were treated with recombinant TGFβ1 (0.3 ng/mL) (R&D Systems) and **4-AuNC** (0.2, 0.4, 0.8, 1.5 or 3 µM). After 24 h of incubation, the media were collected and cells were washed twice with PBS and incubated for 10-15 min with 500 µL of Trypsin at 37 ºC. Unattached cells of each treated group were collected in falcon tubes (15 mL) and counted by bright field microscopy in a Neubauer chamber. Then, media collected from the first incubation and the trypsin solutions containing the cells were treated with 600 µL of 37% HCl and the resultant suspension was sonicated for 60 minutes at 60 ºC. Finally, 4.9 mL of bi-distilled water was added. The Au concentration was determined by measuring the sample using an ICP-MS, NexION 300XX (Perkin Elmer). Results included triplicate of three independent assays of low passage cells (p2).

***In vitro* confocal microscopy imaging.** Internalization of **4-AuNC** were also evaluated using fluorescence confocal microscopy. Primary fibroblast cells were cultured on a µ-

Slide 8-well plate at a density of $2x10^4$ cells per well in 250 µl of complete medium. After 24 h, the growth medium was removed and cells were then incubated with recombinant TGFβ1 (0.3 ng/mL) (R&D Systems) and 0.8 µM of **4-AuNC** for 24 h. Then, the cells were incubated 30 min with MitoTracker™ Red FM for mitochondria staining, washed three times with PBS to remove free unbound **4-AuNC** and finally 250 µL of Opti-MEM medium was added to each well. Cellular uptake of the AuNC was detected using a high-content imaging fluorescent microscope (LSM 880, Carl Zeiss Jena, German). Excitation wavelengths of 405 nm to image the **4-AuNC** and 581 nm to image the mitochondria were used for all the confocal fluorescent microscopy experiments. Intracellular focal plane independent images as well as intracellular z-stacks were taken from samples incubated 24 h with **4-AuNC**. Z-stacks images were projected using ImageJ software.

Functional luciferase refolding assay

Thermally denatured luciferase (1.5 µg/ml of protein at 46 °C for 10 min) was added to myocardial primary fibroblast lysates incubated with increasing concentrations of **4-AuNC** (0.1, 0.2, 0.4, 0.8, 1.5, 3.0 µM) and TGFβ (0.3 ng/ml for 24 h) in 96-well clear bottom plates. Once luciferase is renatured after 2 h incubation at room temperature, Luciferase Assay Reagents (E1501, Promega) were added to catalyze the luminescent reaction. The negative control utilized corresponded to the substrate (heat-denatured luciferase) in the absence of Hsp90 and the positive control corresponded to rabbit reticulocyte lysate (RRL) with high content of Hsp90. Light emission was recorded with a 1 s integration time using a Berthold Centro LB 960 plate reader 3 min after addition of the luminescent reagent. Results included triplicate of three independent assays. Assay procedure, buffers and reagents were previously described more in detail by Eachkoti *et al*.[8]

Animal Studies

Adult (16–20 weeks old) C57BL6 wild type (WT) mice were housed in a 22°C room with 12:12 h light/dark cycle and provided with food and water ad libitum. Mice were divided into 4 groups of n= 3 mice per group: WT, WT + **4-AuNC**, WT+Ang II, and WT+Ang II+ **4-AuNC**.

Live animal studies were approved by the University of Cantabria Institutional Laboratory Animal Care and Use Committee in compliance with the Guide for the Care

and Use of Laboratory Animals (ILAR, 1985) and were conducted in accordance with the "European Directive for the Protection of Vertebrate Animals Used for Experimental and Other Scientific Purposes" (European Communities Council Directive 86/606/EEC).

Mice were placed on preheated pad set to prevent hypothermia and were anesthetized using 5 µl/g of mouse weight of medetomidine (0.2 mg/ml), ketamine (16 mg/ml), and buprenorphine (0.018 mg/ml). Under this anesthesia conditions we performed the following actions:

Subcutaneous implantation of osmotic minipumps

The osmotic minipumps containing Ang II or saline serum (sham) were implanted subcutaneously to anesthetized mice with 5 µl/g of mouse weight of medetomidine (0.2 mg/ml), ketamine (16 mg/ml), and buprenorphine (0.018 mg/ml), through a mid-scapular incision that create a subcutaneous pocket in the dorsum of the neck to infuse a dose of Ang II (1.5 mg/kg per day) or PBS (vehicle) at a delivery rate of 0.25 µl/h for 14 days (Alzet microosmotic pump 1002). These groups of mice are named as "Ang II" and "Sham". The wound was closed with a suture. Mice were monitored daily for any discomfort and they were euthanized 2 weeks after surgery. Mouse body weights were recorded before the animals were euthanized. At the end of the study, all the animals were euthanized, and the hearts were dissected and weighed to compute the ratio of heart weight to body weight (HW/BW, mg/kg). Heart (atrium and left ventricle), aorta, liver, brain, cerebellum, skin, lungs, spleen, intestine, renal tissue, and urine were quickly harvested, flash frozen and stored at −80 °C until assays of gene and protein expression analyses, or embedded in 4% paraformaldehyde for histological analysis. Blood was collected, immediately centrifuged at 3000 rpm at room temperature for 30 minutes and separate the plasma from the cellular content and stored at -80ºC.

4-AuNC intraperitoneal administration

Mice received intraperitoneal (IP) administration of the **4-AuNC** (200 µl of 1 mM) or saline serum (vehicle). These groups of mice are named as "**4-AuNC**" and "vehicle". For the **4-AuNC** IP administration mice were anesthetized using 5 µl/g of mouse weight of medetomidine (0.2 mg/ml), ketamine (16 mg/ml), and buprenorphine (0.018 mg/ml). Mice did not present any sign of discomfort. Mice were weighted and then euthanized at

3 hours, 4 days or 8 days after **4-AuNC** n= 3. Pictures of all hearts were taken, then weighted them and kept frozen until the assays were performed.

4-AuNC biodistribution by ICP-MS

The mice were sacrificed at 8 days post-injection. Organs, tissues of interest and fluids were frozen. The plasma and blood cellular fractions were separated through 30 minutes, 3000 rpm at room T^a centrifugation previous to be frozen. To quantify Au by ICP-MS the samples were weighed and immersed in 2 mL of digestion solution (HNO_3/HCl = 1:3). The dispersions were heated to boiling until organs were completely dissolved. A 1 mL amount of H_2O_2 was then added into the solution, and heating continued until the solution became clear and transparent. The solution was then cooled to room temperature, diluted by 2% HNO_3 to 10 mL, and subsequently analyzed by inductively coupled plasma mass spectrometry ICP-MS to determine the concentration of Au in each sample. All experiments were carried out in triplicate. All the data obtained were plotted and statistically analyzed using the software package GraphPad Prism version 5.0 for Windows. All samples were compared using a one-way ANOVA and Bonferroni post hoc test (* $P < 0.05$, ** $P < 0.01$, and *** $P < 0.001$). Only significant differences among the samples are indicated in the charts.

***Ex vivo* fluorescence imaging (IVIs)**

Ex vivo fluorescence images of the hearts were obtained on an IVIS Spectrum fluorescent imaging system from Xenogen (IVIs). The heart was extracted from anesthetized mice with 5 µl/g of mouse weight of medetomidine (0.2 mg/ml), ketamine (16 mg/ml) and buprenorphine (0.018 mg/ml). **4-AuNC** or saline vehicle injections were administrated to the extracted mice hearts. The heart injections were performed through the left ventricle apex (20 ul of 1mM). Right after the injections the hearts were placed into the IVIS chamber. Excitation and emission values for **4-AuNC** visualization were established at 440/520 nm using a 1 mM **4-AuNC** stock. The exposure time set in "auto-expose" and the acquired images were analyzed using the Live Image 4.7.2 software.

Assessment of myocardial fibrosis by both partial and complete Masson's trichrome staining

The histological assessment of myocardial fibrosis was performed by the complete Masson's trichrome staining (SIGMA ALDRICH). The hearts were isolated and fresh

frozen after incubation in sucrose 30% for 24 hours. The degree of fibrosis was detected in 50 μm cross sections that were the same or consecutive slices to the ones used for the SXRF analysis.

The stained myocardial cross sections were placed on an upright fluorescence microscope (Eclipse 80i, Nikon) to acquire the bright field images using a 20x 0.5 NA or 40x 0.57 NA objective, a DS-Ri1 color camera (1280x1024 pixels; 0.46μm & 0.23μm pixel size).

The partial Masson's trichrome staining was utilized to detect fibrosis by the exposure of Tungsten and subsequent detection by SXRF analysis. Tissue sections were incubated in a 1:1000 dilution from the original Phosphotungstic/Phosphomolybdic acid Solution (SIGMA ALDRICH) for 5 minutes, wash (H_2O) to remove the excess and cover by a 30% sucrose solution layer for its preservation.

Determination of mRNA expression by Q-PCR

The total RNA was obtained with TRIzol® reagent (Gibco BRL, Grand Island, NY). Complementary DNA was prepared from 0.5 μg total RNA by random priming using a first-strand cDNA synthesis kit (Promega Corp). Primers sequence for the Sybr green Q-PCR of COL Ia1, COL IIIaI, FN, Hsp90α, Hsp90β, Nppa, Nppb were: COL Ia1 forward: TGGGGCAAGACAGTCATCGAATA; reverse: GGGTGGAGGGAG TTTACACG. COL IIIa1 forward: ACCCCATGATGTGTTTTGTGGCA; reverse: CAGGTCCTCGGAAGCCACTA. FN forward: CACCCACATGGCAGCTCACA; revers: ATGGGAACCCTGAAGCCAGC. Hsp90α forward: TTCCAGAAGATG AAGAGGAAAA; reverse: GTCACCAGTCGGTTTGACAC. Hsp90β forward: TCTACTTCATGGCTGGGTCA; reverse: AACTCGGGAAGAGCCTGAAT. Nppa forward: GGCAGAGACAGCAAACATCA; reverse: GTCCCAGTCTGTGTCC CACT. Nppb forward: CAGCTCTTGAAGGACCAAGG; reverse: AGGGAAGTGGC AAGGTAGGT. The target mRNA expression levels were normalized to 14S levels, 14S forward: AGTGACTGGTGGGATGAAGG; reverse: CTTGGTCCTGTTTCCTCC TG. Relative quantization was expressed as fold-induction compared with control 14S in duplicate.

Determination of protein expression levels by Western Blot

Tissue samples were disrupted and lysated. Western blot analysis using 10% sodium dodecyl sulfate-polyacrylamide (SDS-PAGE) gel and transferred onto polyvinylidene

difluoride (PVDF) membranes (Bio-Rad Lab., California, USA) determined fibrotic-related protein expression and their correspondent densitograms (bands density measurements using Image-J software) were used to quantify differences in expression. The primary antibodies used were: polyclonal anti αRSK (Santa Cruz); and polyclonal anti COL III and FN (Santa Cruz). 4-AuNC antibody was purified from rabbits immunized by CTPR390 protein (1) (antibody platform from Unidad de Ensayos Biotecnológicos y Biomédicos, Servicios Científico Técnicos, Universidad de Oviedo, Spain). Secondary antibodies conjugated with IRDye 800CW and IRDye 680RD were used for immunodetection and infrared fluorescence detection with Odyssey® Imaging Systems.

SXRF experiments

SXRF experiments were performed at the I18 beamline at the Diamond Synchrotron Light Source (Oxford, UK). 4 animal groups (WT, WT+ **4-AuNC**, WT+Ang II, and WT+Ang II+ **4-AuNC**) were treated with **4-AuNC** (0 or 300 mg/kg) for different times (3h, 4d or 8d). After **4-AuNC** treatment, mice hearts were isolated and fixed with paraformaldehyde (4% in PBS) for 48 h, cryo-protected using 20% sucrose solution for 1.5 days, embedded in cryo-molds using OCT, and stored at -80ºC until sectioned. 20-50 μm thick heart sections were generated and deposited on sapphire discs, and studied using SXRF mapping in I18. Irradiation of the samples was carried out using a beam focused at 5x5 μm^2, and energy fixed to 13 keV (flux between 2.5-3.0x10^{11} ph/s). Detection was performed using two 4-element Vortex silicon drift detectors (Hitachi). Scan step size was fixed at 50x50 μm^2 (dwell time 0.5 s) for coarse scans to optimize the measurement parameters. Following this, high resolution SXRF elemental maps were collected in 500x500 μm^2 regions of interest on different areas of the hearts studied (septum, top, and bottom) using 5x5 μm^2 scan steps (dwell time 1 s). The raw maps were processed using the free PyMCA software.[9] Concentration maps were produced assuming a matrix of 20 or 50 μm thick soft tissue, while the quantitative calibration was determined using a thin film x-ray fluorescence 7-element reference sample (AXO Dresden GmbH; SI Appendix, Table S3). The concentration maps were further processed using FIJI ImageJ package with the EDFread plugin.[10]

Results and discussion

Control experiments for the synthesis and stabilization of AuNC

The $C2_{NC}$ module **[2]** was tested for its ability to stabilize gold nanoclusters, using a slightly modified green biocompatible chemistry method that had been previously described,[5] in the context of a protein with two flanking wild type CTPR repeats **[3]** (Figure S1A), since a CTPR with two repeats is marginally stable.[11] In order to ensure that the fluorescence emitters were **3-AuNC**, a complete set of control experiments were carried out (Figure S1). It is clear that the presence of the protein **3** was essential for the stabilization of AuNC, and also that the sodium ascorbate is needed for the reduction of Au salts, given that fluorescence emission was observed only when all the reagents were present (Figure S1B).

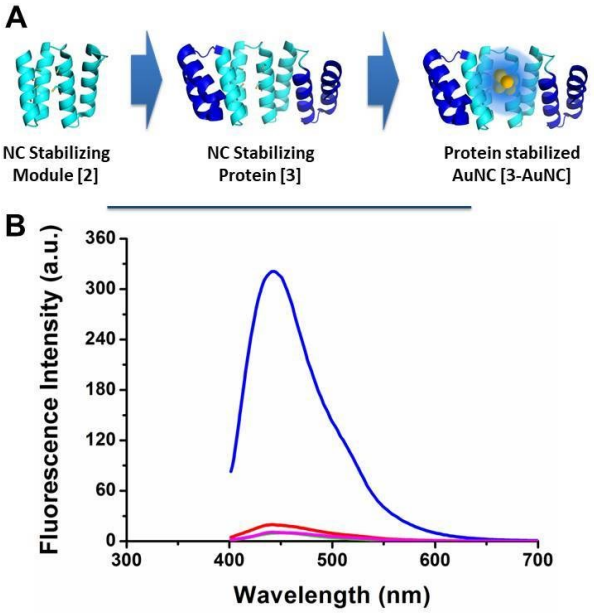

Figure S1. (**A**) General scheme of the protein scaffold design and the synthesis and stabilization of fluorescent AuNC. A nanocluster stabilization site is introduced on a modified CTPR module in which four cysteines have been introduced **[2]** (cyan) on the structure of CTPR (PDB ID: 2HYZ).[12] Designed protein **[3]** made by the fusion of the wild type (blue) and **2** (cyan) modules. (**B**) Fluorescence emission spectra of the complete reaction of **3-AuNC** (blue line), the protein in the presence of the Au salt (red line), the protein **3** in the presence of sodium ascorbate (magenta line) and the Au salt in the presence of sodium ascorbate (green line).

Time-resolved Fluorescence Measurements

Analysis of PL decay data was carried out with Fluofit (Picoquant). The emission intensities (I) were best fit to a tri-exponential decay over time (t): $I(t) = A1 \exp(t/\tau1) + A2 \exp(t/\tau2) + A3 \exp(t/\tau3)$ in which A1, A2, A3, τ1, τ2 and τ3 are respectively the amplitudes and lifetimes of the three emission components. Reduced chi-square value ($\chi2$) of 1.036906 was obtained for **4-AuNC**. The results are shown in Figure S2. Multi-exponential fits of the photoluminescence decay curves, provided 2.53 ns amplitude-weighted average lifetimes. It is noted that lifetimes in this range are characteristic of transitions between singlet states in AuNC.[13-15]

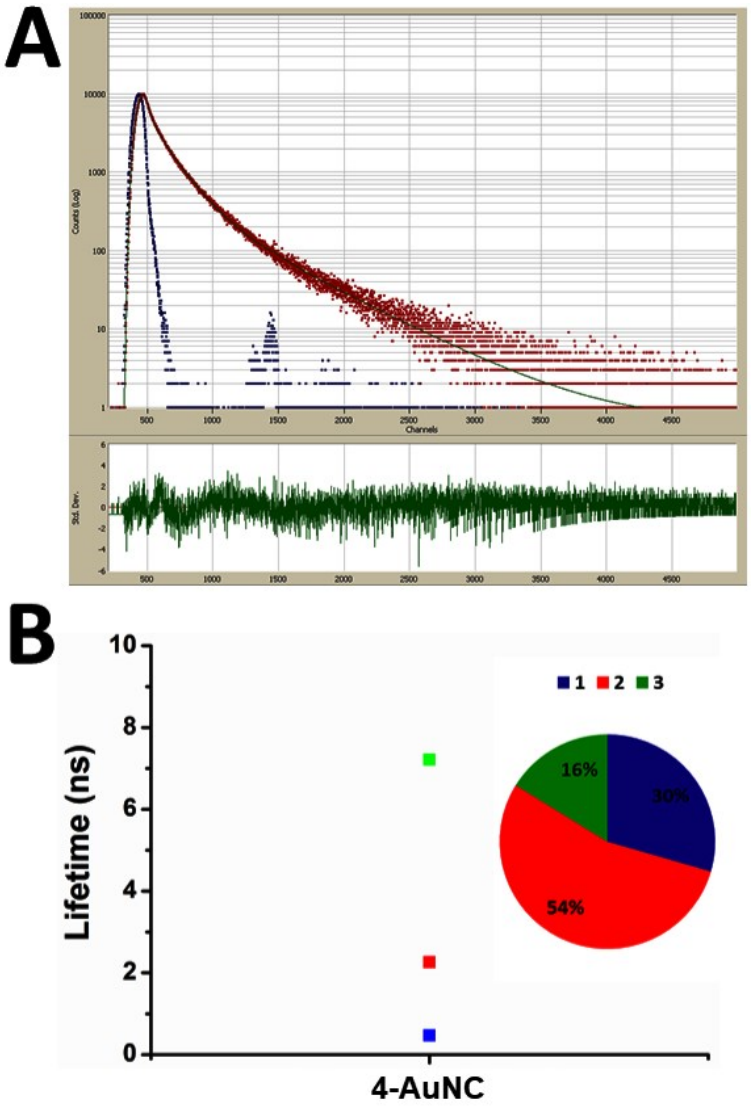

Figure S2. The fluorescent lifetime analysis **4-AuNC**. (**A**) PL decay curve with corresponding three-exponential fits depicted by a solid green line. (**B**) Corresponding lifetime components and their statistical weights for **4-AuNC**. Amplitude-weighted average lifetimes are displayed.

X-ray photoelectron spectroscopy (XPS)

The XPS spectrum of **4-AuNC** showed a peak at the binding energy of 84.6 eV (Au 4f7/2), which is between the typical binding energies of Au foil (84.0 eV) and Au(I)-L3 complex (86.0 eV) (Figure S3). This result suggests that both Au(0) and Au(I) coexist in the **4-AuNC**, as has been previously observed for some gold NC.[16] To further determine the Au oxidation states, the quantitative deconvolution of the Au 4f7/2 peak was performed. It could be well-deconvoluted into Au(I) and Au(0) components with binding energies of 84.5 and 83.5 eV, respectively (Figure S3). On the basis of the area ratio between these two peaks, the Au(0):Au(I) ratio was determined to be about 1:2.

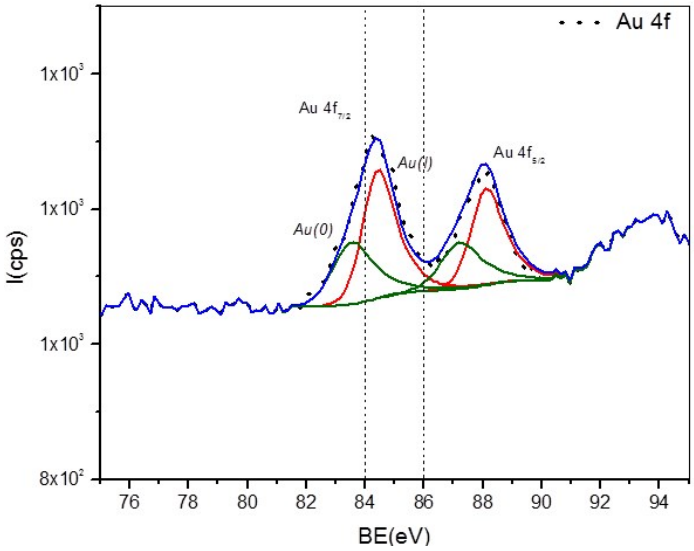

Figure S3. XPS spectrum of **4-AuNC**.

Matrix assisted laser desorption ionization (MALDI) mass spectrometry

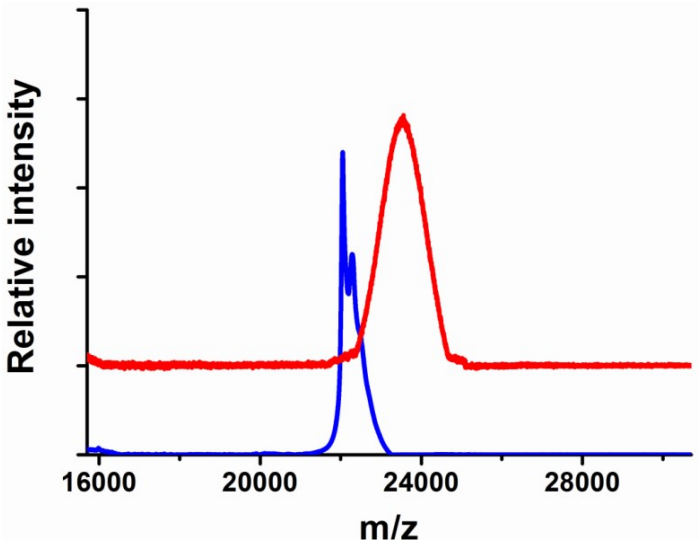

Figure S4. MALDI-TOF mass spectra of **4** protein (blue line) and **4-AuNC** (red line).

Determination of the number of Au atoms in the 4-AuNC

MALDI-TOF was used to determine the number of Au atoms in the **4-AuNC**. AuNC presented certain polydispersity in size (Table S1).

Table S1. Determination of the number of Au atoms in the **4-AuNC** by MALDI-TOF.

Sample	MALDI-TOF		
	MSC[a]	FWHM[b]	NMA[c]
4	21981.25	351.51	--
4-AuNC	23557.52	1617.08	4-12

[a]Center of mass peak in Daltons (MSC). [b] Full width at half maximum in Daltons (FWHM). [c] Number of metal atoms per cluster (NMA).

Inductively coupled plasma mass spectrometry (ICP-MS)

100 µL of the FPLC purified **4-AuNC** at 100 µM concentration was mixed with 300 µL of 37% HCl and the resultant suspension was sonicated for 30 minutes at 40ºC. Finally, 2700 mL of bi-distilled water was added. The Au concentration of the FPLC purified **4-AuNC** was determined by measuring the sample ICP-MS (Table S2). The protein concentration of the FPLC purified AuNC was measured by Bradford assay.

Table S2. Quantification of Au atoms per protein by ICP-MS.

Protein concentration [µM]	Metal concentration [µg/L] / [µM]	Number of Au atoms per protein
100	157619±9850 / 800±50	8±1

Scanning Transmission Electron Microscopy (STEM)

The morphology and size of the **4-AuNC** was evaluated by scanning transmission electron microscopy (STEM), taking advantage of the chemical contrast of Au obtained in high-angle annular dark field (HAADF). Indeed, **4-AuNC** showed NC diameters of 1.0 ± 0.2 nm (Figure S5). This size regime is accordant with the size range of previously reported blue-emitting AuNC.[17, 18] However, the **4-AuNC** visualized in the STEM images seemed larger than those obtained from the MS analysis, as the larger metal AuNC observed in the STEM images are difficult to ionize and cannot be detected by the MS.[19, 20]

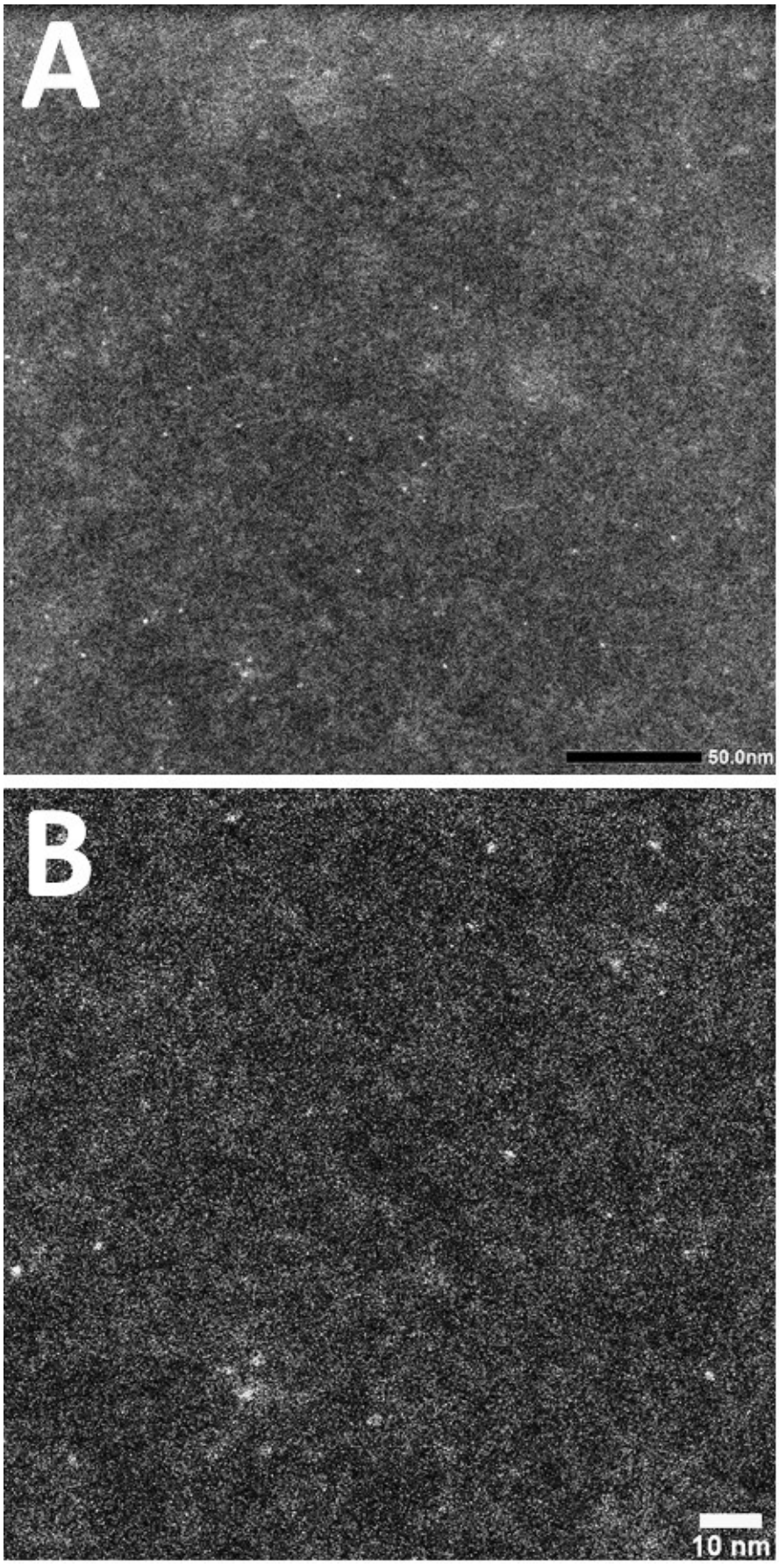

Figure S5. HAADF STEM images of the purified **4-AuNC**.

Multifunctional 4-AuNC hybrid nanomaterial stability

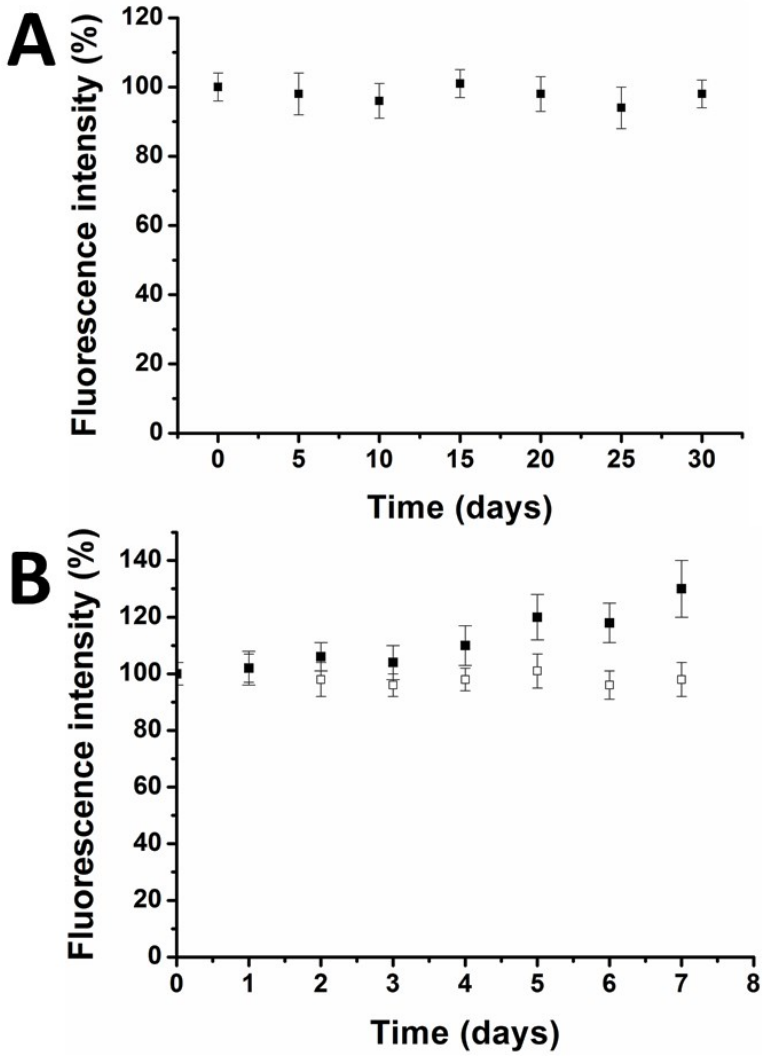

Figure S6. Multifunctional **4-AuNC** hybrid nanomaterial stability. (**A**) **4-AuNC** stability in PBS during 30 days at 4°C. (**B**) **4-AuNC** stability evaluated in physiological conditions PBS (empty squares) and Human plasma (black squares) during 8 days at 37ºC.

***In vitro* cytotoxicity assays**

The biocompatibility of the **4-AuNC** was evaluated in NIH-3T3 fibroblast cell line (Figure S7A) and primary cardiac fibroblasts extracted from adult mice (Figure S7B) at different concentrations of **4-AuNC** under standard cell culture conditions. Figure S7 showed that the multifunctional **4-AuNC** hybrid nanomaterial did not present any evident cytotoxicity even at the highest concentration tested.

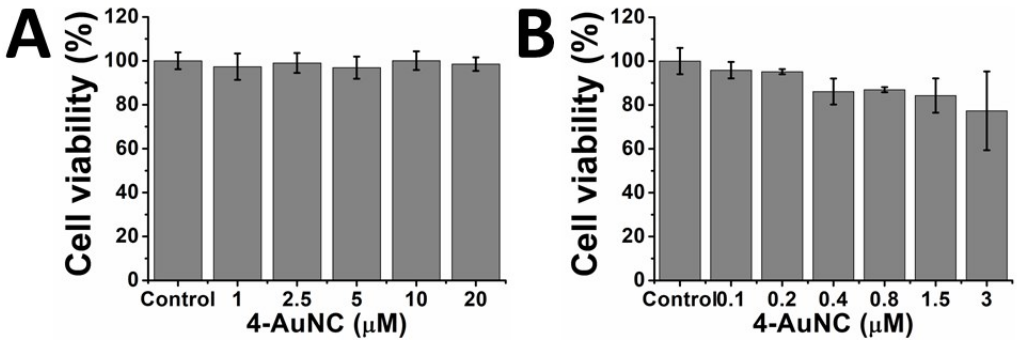

Figure S7. Cytotoxicity of the **4-AuNC** on NIH-3T3 fibroblast cells (**A**) primary cardiac fibroblasts (**B**) measured by Alamar blue assay after 5 days of incubation.

Functional assays in myocardial cultured primary fibroblasts

Having demonstrated that significant reduction of collagens I and III is possible in fibroblasts treated with the **1** protein lacking AuNC,[21] the effect of multifunctional **4-AuNC** hybrid nanomaterial on myocardial fibroblasts was assessed (Figure S8). The gene expressions for the main pro-fibrotic structural fiber proteins (COL I, COL III and FN) were analyzed after **4-AuNC** treatment obtaining a significant reduction on their transcript levels, comparable with the results obtained with **1** protein without AuNC.[21]

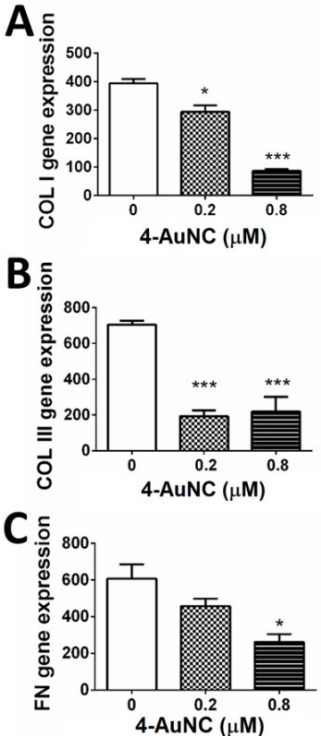

Figure S8. A, B, C: Gene expression of collagen I (COL I), collagen III (COL III**)** and Fibronectin (FN) in myocardial primary fibroblasts treated with **4-AuNC**. Primary fibroblasts were activated with TGFβ (0.3 ng/ml) and data were collected 24 hours later. Data were expressed as mean ± SD in arbitrary units (*$p < .05$, ***$p < .001$; Mann–Whitney test).

In vitro internalization of multifunctional 4-AuNC hybrid nanomaterial

In order to assess the *in vitro* internalization of **4-AuNC**, ICP-MS measurements were carried out on primary fibroblasts incubated with **4-AuNC** (0.1, 0.2, 0.4, 0.8, 1.5, 3.0 μM) for 24 h, washed several times and lysed. The results showed that cells treated with **4-AuNC** seemed to accumulate Au in a dose-dependent manner (Figure S9A). These results represent a total internalization of 14±3% (average cell internalization at 6 different **4-AuNC)**.

The *in vitro* **4-AuNC** internalization was also evaluated by live confocal microscopy studies thanks to the excellent fluorescent properties of the **4-AuNC**. Cells were incubated with recombinant TGFβ1 (0.3 ng/mL) and 0.8 μM of **4-AuNC** for 24 h. Then, cells were washed three times with PBS to remove free unbound **4-AuNC** and the cells were incubated 30 min with MitoTracker™ Red FM for mitochondria staining in 250 μL of Opti-MEM medium. Finally, cells were imaged by live confocal fluorescence microscopy (Figure S9B and Supporting video files). Images of intracellular focal planes acquired after 24 h of incubation with 0.8 μM of **4-AuNC** showed dotted fluorescence in the cytoplasm, compared to non-treated cells which, as expected, did not show any fluorescence. These results clearly demonstrate the internalization of **4-AuNC** into the primary fibroblasts (Figure S9B and Supporting video files).

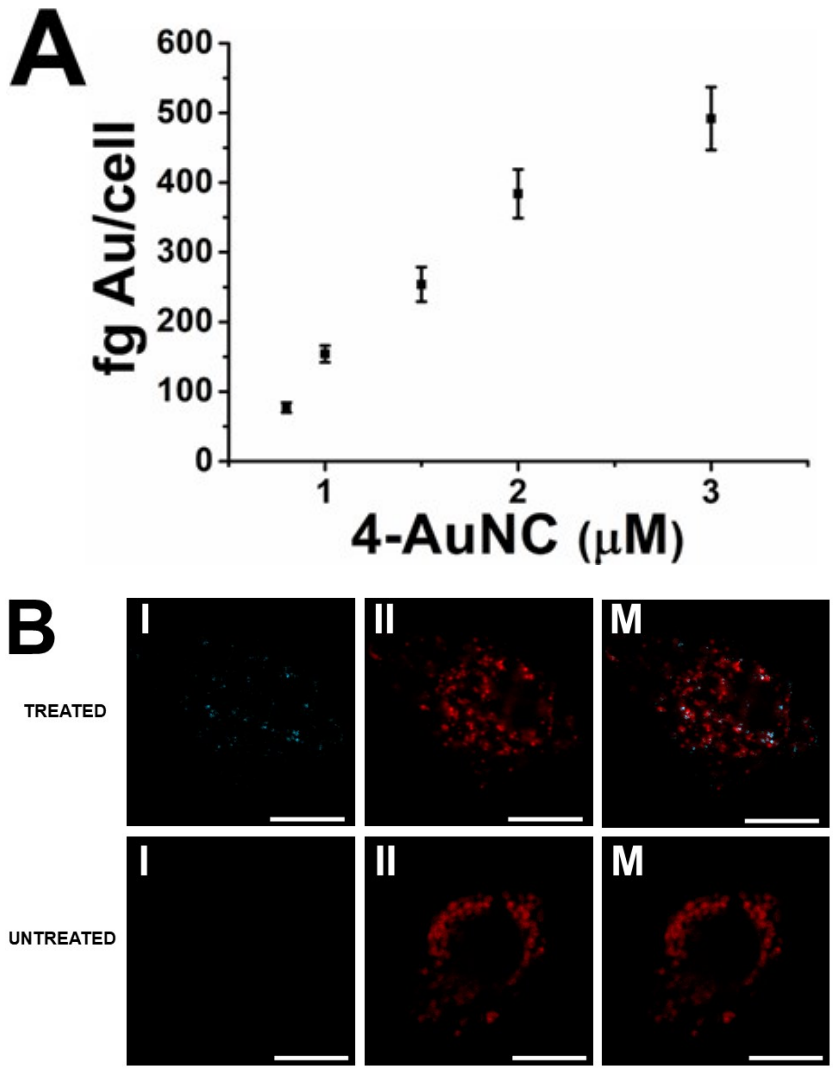

Figure S9. *In vitro* internalization of **4-AuNC** in primary cardiac fibroblasts. **A.** *In vitro* internalization measured by ICP-MS (femtograms per cell). **B.** Confocal microscopy images from primary cardiac fibroblasts incubated with (treated) and without (untreated) **4-AuNC** after 24 h. Two different channels: I. Blue fluorescence of 4-AuNC, and II. MitoTracker™ Red FM for mitochondria staining. M. shows the merged image. Scale bars = 10 μm.

***In vitro* evaluation of the Hsp90 folding capabilities under 4-AuNCs treatment**

In order to verify if the treatment with the multifunctional **4-AuNC** hybrid nanomaterial caused any inhibition of the Hsp90 chaperone activity, essential for maintaining the activity of several signaling proteins, a functional luciferase refolding assay was performed in myocardial primary fibroblast lysates treated with increasing concentrations of **4-AuNC** (0.1, 0.2, 0.4, 0.8, 1.5, and 3.0 μM) and TGFβ (0.3 ng/ml) for 24 h. Figure S10 shows that the multifunctional **4-AuNC** hybrid nanomaterial did not inhibit the Hsp90 chaperone activity even at the highest concentration tested. These results were in agreement with previous studies using the protein **1.**[22]

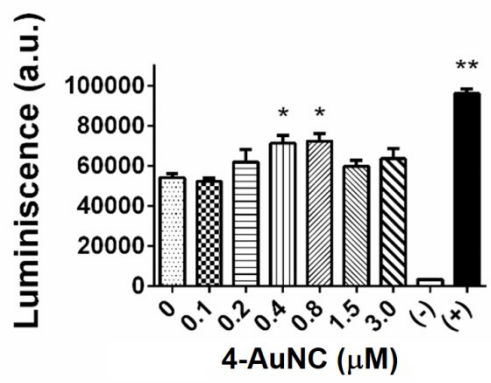

Figure S10. Hsp90-dependent refolding activity in cell lysates of primary fibroblasts containing increasing concentrations of **4-AuNC** in the presence of heat denatured luciferase (Hsp90 substrate). Data were expressed as mean ± SD in arbitrary units (a.u.) (*p < .05, **p < .005; Mann–Whitney test).

Myocardial remodeling reduction

In addition to the *in vivo* monitoring of cardiac fibrosis reduction, at molecular level, by **4-AuNC** treatment, a study of cardiac hypertrophy (heart weight to body weight ratio) was performed. After 8 days of the **4-AuNC** treatment the myocardial hypertrophy was notably reduced in comparison with the fibrotic control (Ang II+Veh), thus indicating a reduction of hypertrophy and fibrosis (Figure S11). However, at a shorter time after **4-AuNC** treatment (3 hours) was not observed any reversion of the hypertrophy (Figure S11).

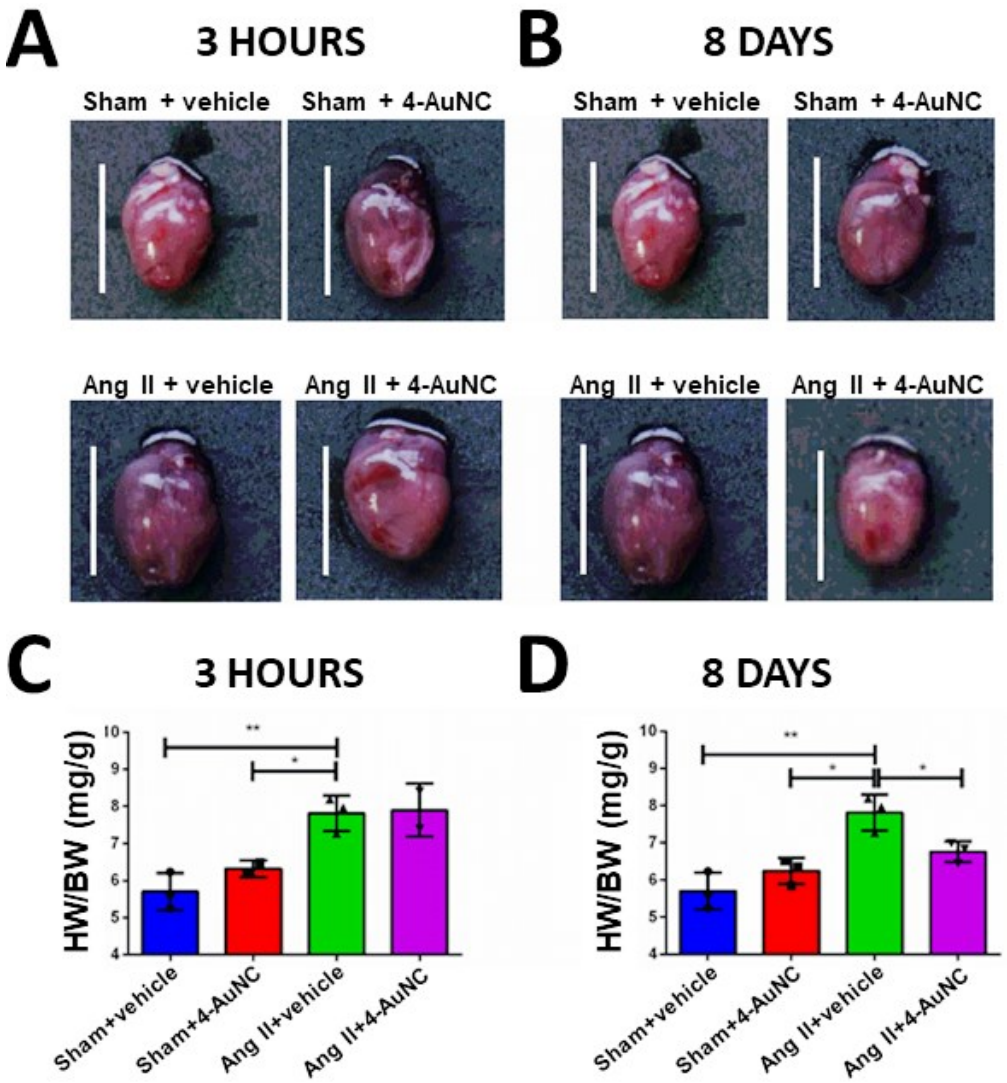

Figure S11. Representative photographs of the hearts of healthy (Sham) and fibrotic (Ang II) mice treated with **4-AuNC** and their correspondent controls (Sham+**4-AuNC**, Ang II+**4-AuNC** and Sham+vehicle, Ang II+vehicle) at 3 hours (**A**) and 8 days (**B**) after treatment. White vertical bar indicating 2 cm. Quantification of heart relative weight (HW/BW) ratio at 2 time points (3 hours (**C**) and 8 days (**D**) after **4-AuNC** injection). Data were expressed as mean ± SD of the heart weight (mg) /Body weight (g) (HW/BW (mg/g)). (*p < .05, **p < .005; Mann–Whitney test).

***In vivo* 4-AuNC biodistribution by ICP-MS**

ICP-MS allowed assessing the *in vivo* biodistribution of **4-AuNC** in mice 8 days after a single injection (200 µl at 1mM) of the multifunctional **4-AuNC** hybrid nanomaterial. Figure S12 shows that **4-AuNC** was accumulated mostly in the kidney, liver, and spleen of both healthy and fibrotic individuals. On the contrary, **4-AuNC** was found in low quantities in the stomach, lung, intestine, urine, and blood, and was not detected in brain and cerebellum. Interestingly, significant differences between healthy and fibrotic individuals were observed in the accumulation of **4-AuNC** in the cardiovascular organs,

such as atria, right and left ventricles, and aorta (Figure S12), which have consistently been detected as damaged areas in Ang II *in vivo* models.[23, 24]

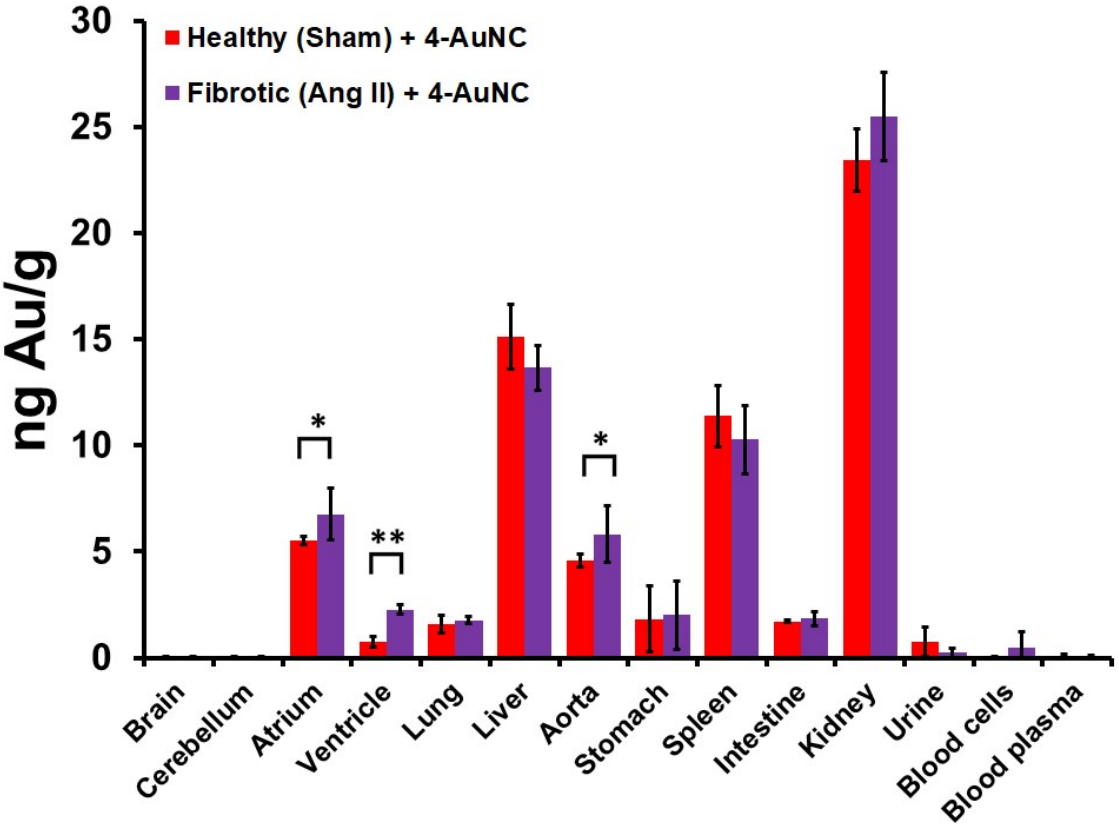

Figure S12. *In vivo* biodistribution of **4-AuNCs** in healthy (Sham) and fibrotic (Ang II) mice determined by ICP-MS. Au measurements performed 8 days after the **4-AuNC** injection. Data with standard errors from n = 3. (*p < 0.05, **p < 0.01).

XRF imaging of heart sections

SXRF using microfocused synchrotron radiation allowed to quantify the accumulation of Au in tissue samples, while providing lateral resolution not available from ICP-MS. In order to assess the specific localization of **4-AuNC** in the hearts of fibrotic (Ang II) and healthy (sham), first the calibration of the instrument was performed using a reference sample (Table S3). Then, Au elemental maps of the tissue samples were acquired using SXRF (Figure S13-24). Figure S13 shows an example of the SXRF spectrum from a section of a Fibrotic (Ang II) heart obtained from a mouse 8 days after **4-AuNC** treatment.

Table S3. Elemental area density of a 7-element RF4-200-S1749 reference sample (according to the supplier, AXO Dresden GmbH). The calibration was done at 13 keV excitation energy using a beam focused at 2x2 μm^2 (Scan step size 5x5 μm^2; dwell time 1s).

Element	Mass (ng/mm^2)
Pb	7.61±0.96
La	11.01±0.62
Pd	1.8±1.0
Mo	1.32±0.4
Cu	2.84±0.35
Fe	5.04±0.87
Ca	19.31±1.10

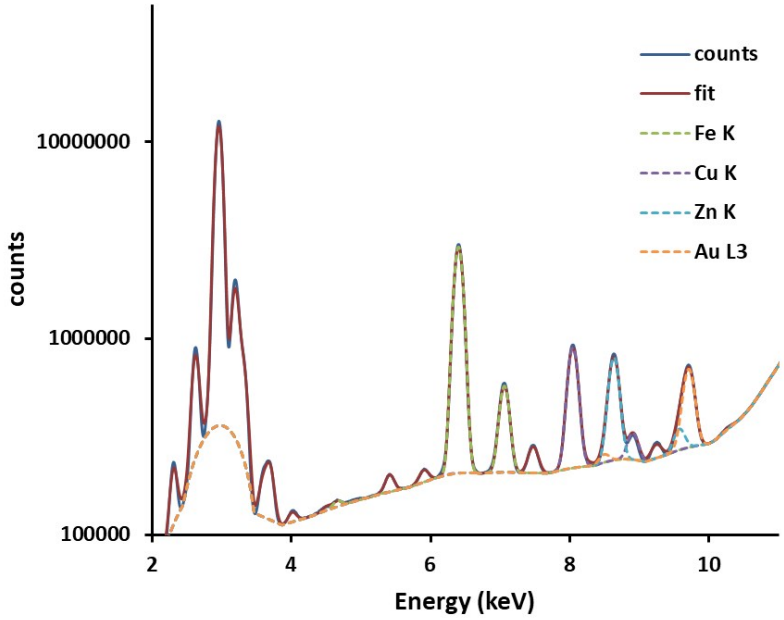

Figure S13. SXRF spectrum from a Fibrotic (Ang II) heart-cross section obtained from a mouse 8 days after **4-AuNC** treatment; Raster scan: 5x5 μm^2 step size, 1 s dwell time. The spectrum was fitted using PyMca,[9] and the contribution of selected elements is displayed: Fe, Cu and Zn K x-ray emission lines, and Au L x-ray emission lines.

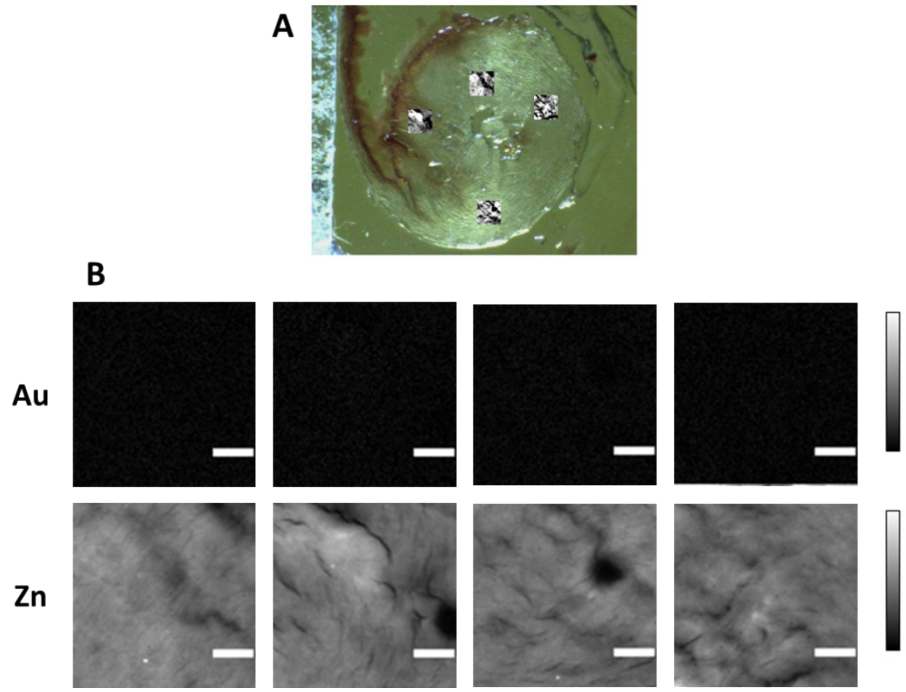

Figure S14. A. Heart section from a vehicle treated fibrotic (Ang II) mouse showing the areas studied with SXRF. **B**. Au L and Zn K SXRF elemental maps showing localization of Au and Zn elements in those areas; Raster scan: 5x5 μm^2 step size, 1 s dwell time. Scale bar 100 μm. Concentration range in images: 0-2 ng mm^{-2} Au or 0-4 ng mm^{-2} Zn.

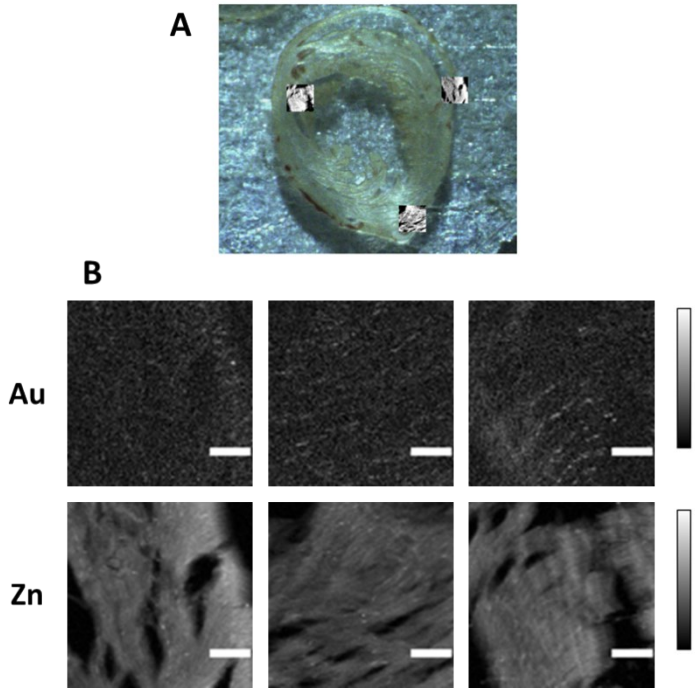

Figure S15. A. Heart section from a fibrotic (Ang II) mouse 3 hours after the **4-AuNC** treatment showing the areas studied with SXRF. **B**. Au L and Zn K SXRF elemental maps showing localization of Au and Zn elements in those areas; Raster scan: 5x5 μm^2 step size, 1 s dwell time. Scale bar 100 μm. Concentration range in images: 0-2 ng mm^{-2} Au or 0-4 ng mm^{-2} Zn.

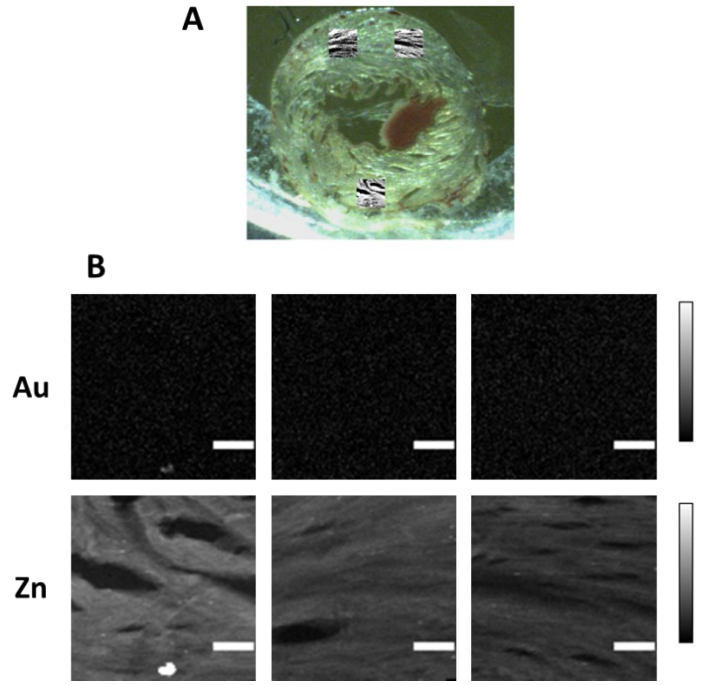

Figure S16. A. Heart section from a healthy (Sham) mouse 3 hours after the **4-AuNC** treatment showing the areas studied with SXRF. **B**. Au L and Zn K SXRF elemental maps showing localization of Au and Zn elements in those areas; Raster scan: 5x5 μm^2 step size, 1 s dwell time. Scale bar 100 μm. Concentration range in images: 0-2 ng mm^{-2} Au or 0-4 ng mm^{-2} Zn.

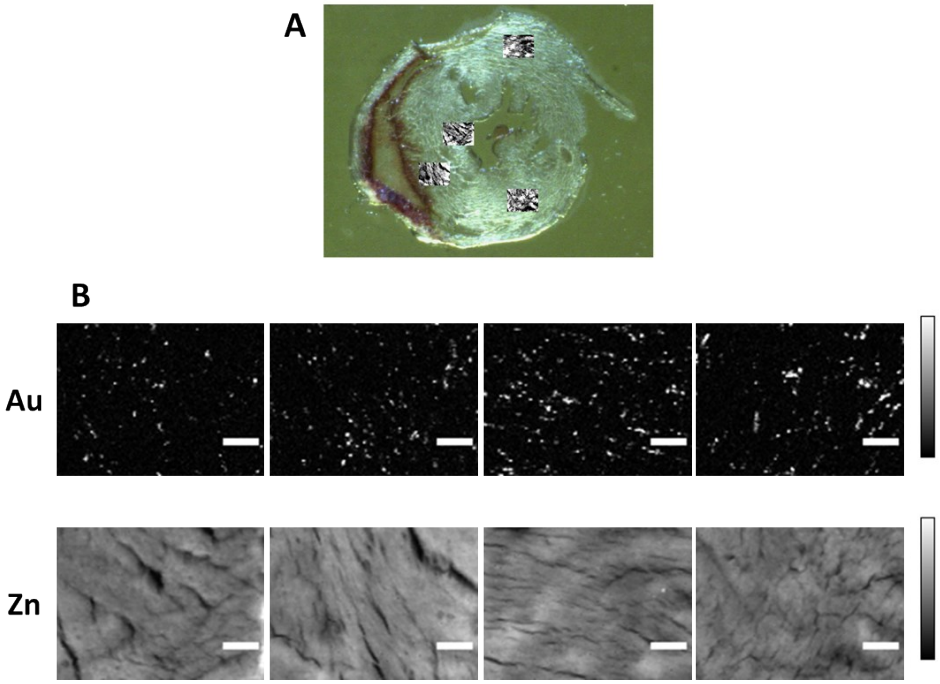

Figure S17. A. Heart section from a fibrotic (Ang II) mouse 4 days after the **4-AuNC** treatment showing the areas studied with SXRF. **B**. Au L and Zn K SXRF elemental maps showing localization of Au and Zn elements in those areas; Raster scan: 5x5 μm^2 step size, 1 s dwell time. Scale bar 100 μm. Concentration range in images: 0-2 ng mm^{-2} Au or 0-4 ng mm^{-2} Zn.

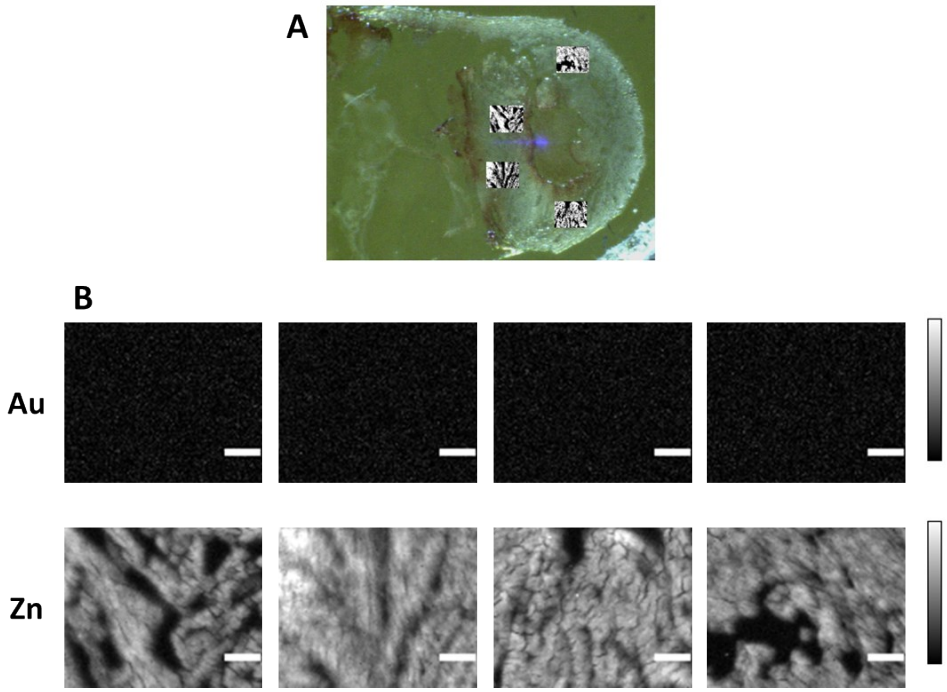

Figure S18. A. Heart section from a healthy (Sham) mouse 4 days after the **4-AuNC** treatment showing the areas studied with SXRF. **B**. Au L and Zn K SXRF elemental maps showing localization of Au and Zn elements in those areas; Raster scan: 5x5 μm^2 step size, 1 s dwell time. Scale bar 100 µm. Concentration range in images: 0-2 ng mm^{-2} Au or 0-4 ng mm^{-2} Zn.

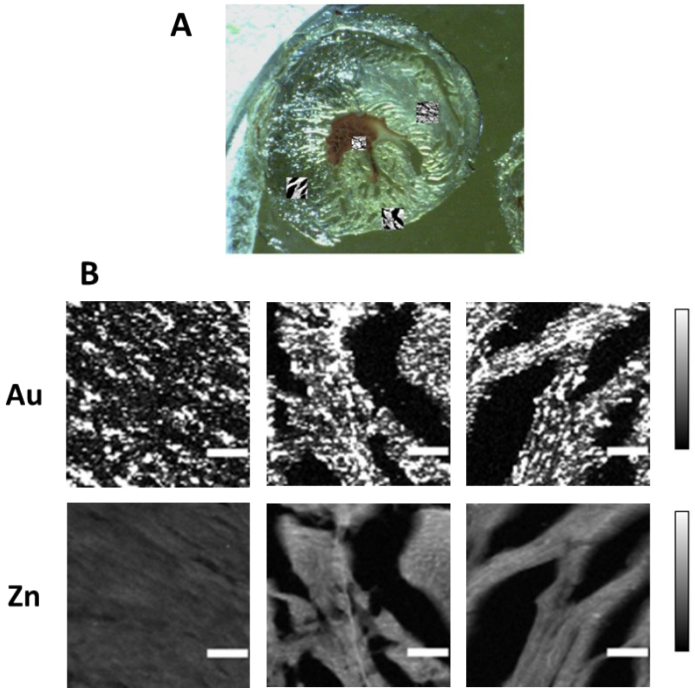

Figure S19. A. Heart section from a fibrotic (Ang II) mouse 8 days after the **4-AuNC** treatment showing the areas studied with SXRF. **B**. Au L and Zn K SXRF elemental maps showing localization of Au and Zn elements in those areas; Raster scan: 5x5 μm^2 step size, 1 s dwell time. Scale bar 100 µm. Concentration range in images: 0-2 ng mm^{-2} Au or 0-4 ng mm^{-2} Zn.

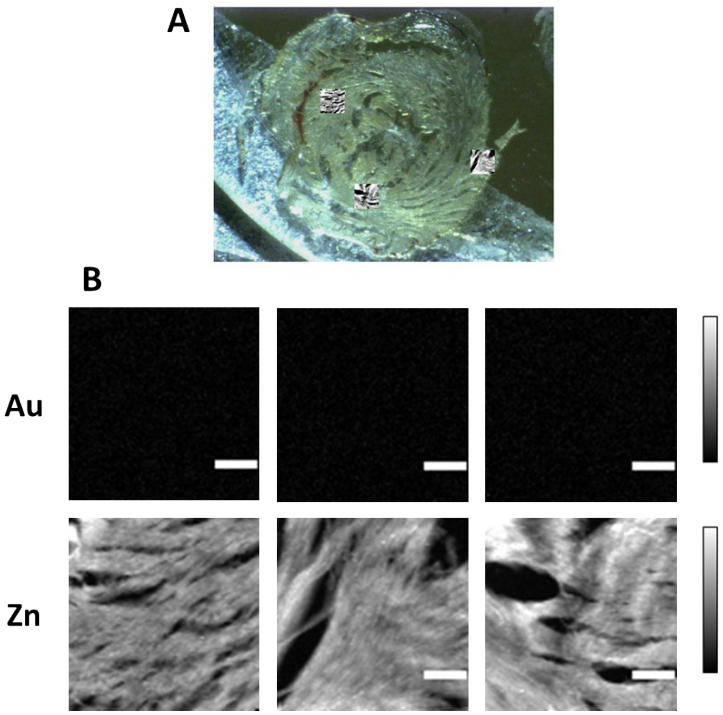

Figure S20. A. Heart section from a healthy (Sham) mouse 8 days after the **4-AuNC** treatment showing the areas studied with SXRF. **B**. Au L and Zn K SXRF elemental maps showing localization of Au and Zn elements in those areas; Raster scan: 5x5 μm^2 step size, 1 s dwell time. Scale bar 100 μm. Concentration range in images: 0-2 ng mm^{-2} Au or 0-4 ng mm^{-2} Zn.

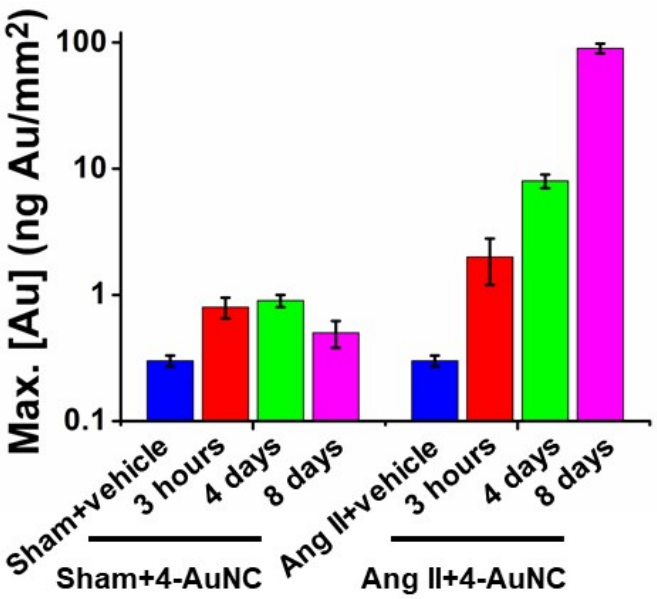

Figure S21. Maximum amount of Au accumulated in a single 5x5 μm^2 region of hearts from fibrotic or healthy mice after different times of the **4-AuNC** treatment. Obtained from heart sections from mice studied with SXRF; Raster scan: 5x5 μm^2 step size, 1 s dwell time. Please note that images in Figure 4, Figures S14-20 and 24 where generated using concentration ranges that saturated the peaks with highest concentration of Au; this was done to show the whole extent of Au accumulation in the different heart samples.

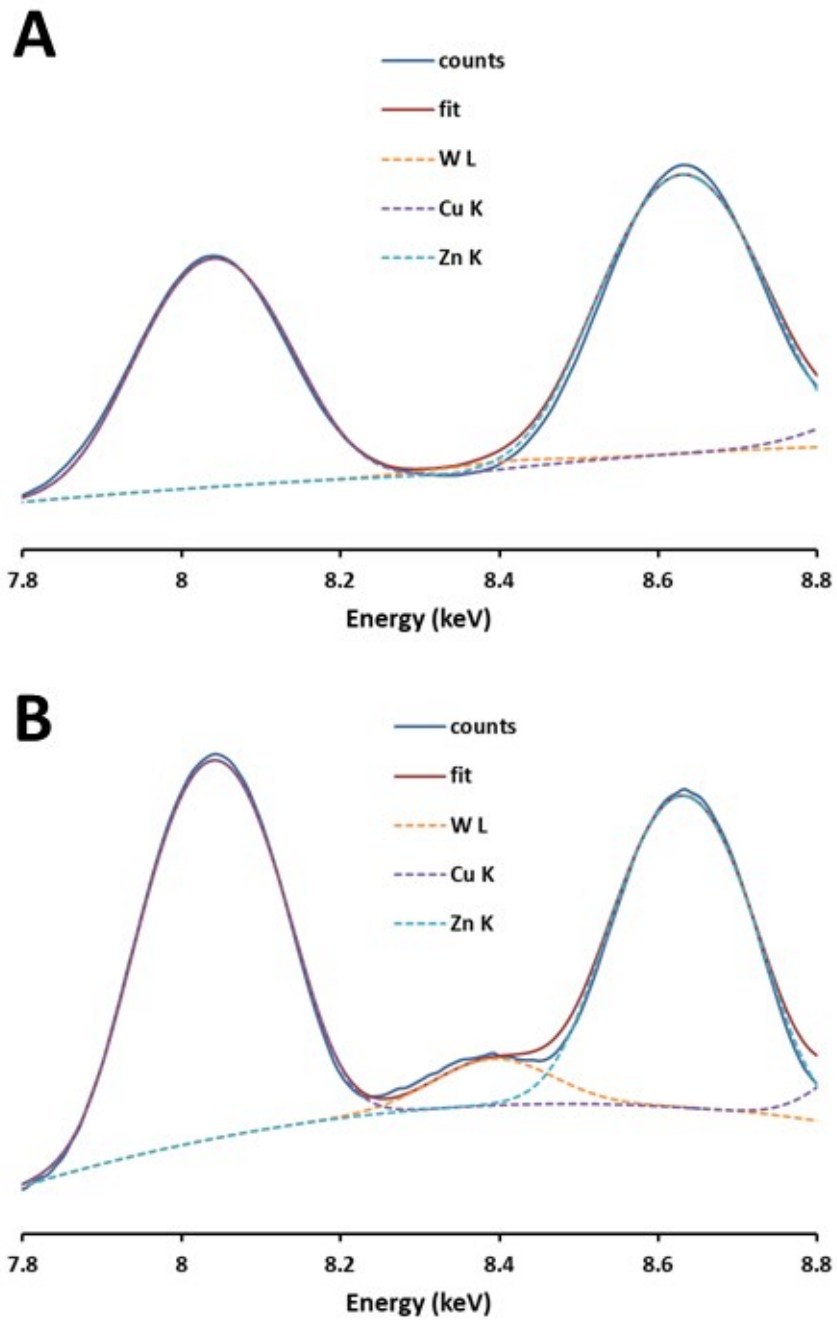

Figure S22. SXRF spectrum from sections of a fibrotic heart obtained from a vehicle treated mouse **A**. not stained with W, and **B**. Tissue sections were incubated in a 1:1000 dilution of Phosphotungstic/Phosphomolybdic acid Solution (SIGMA ALDRICH) for 5 minutes, wash (H_2O) to remove the excess and covered by a 30% sucrose solution layer for its preservation; Raster scan: 5x5 μm^2 step size, 1 s dwell time. The spectrum was fitted using PyMca,[9] and the contribution of selected elements is displayed: Cu and Zn K x-ray emission lines, and W L x-ray emission lines.

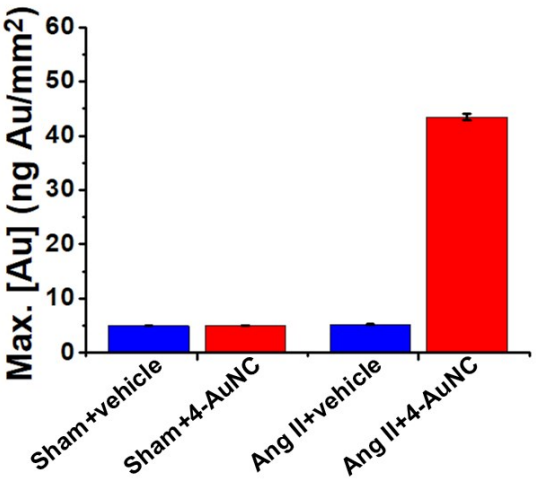

Figure S23. Maximum amount of Au accumulated in a single 5x5 μm^2 region of hearts from fibrotic or healthy mice 8 days after **4-AuNC** treatment. Obtained from heart cross sections of mice incubated with a 1:1000 dilution of Phosphotungstic/Phosphomolybdic acid Solution (SIGMA ALDRICH) for 5 minutes, wash (H_2O) to remove the excess and cover by a 30% sucrose solution layer for its studied with SXRF; Raster scan: 5 x 5 μm^2 step size, 1 s dwell time.

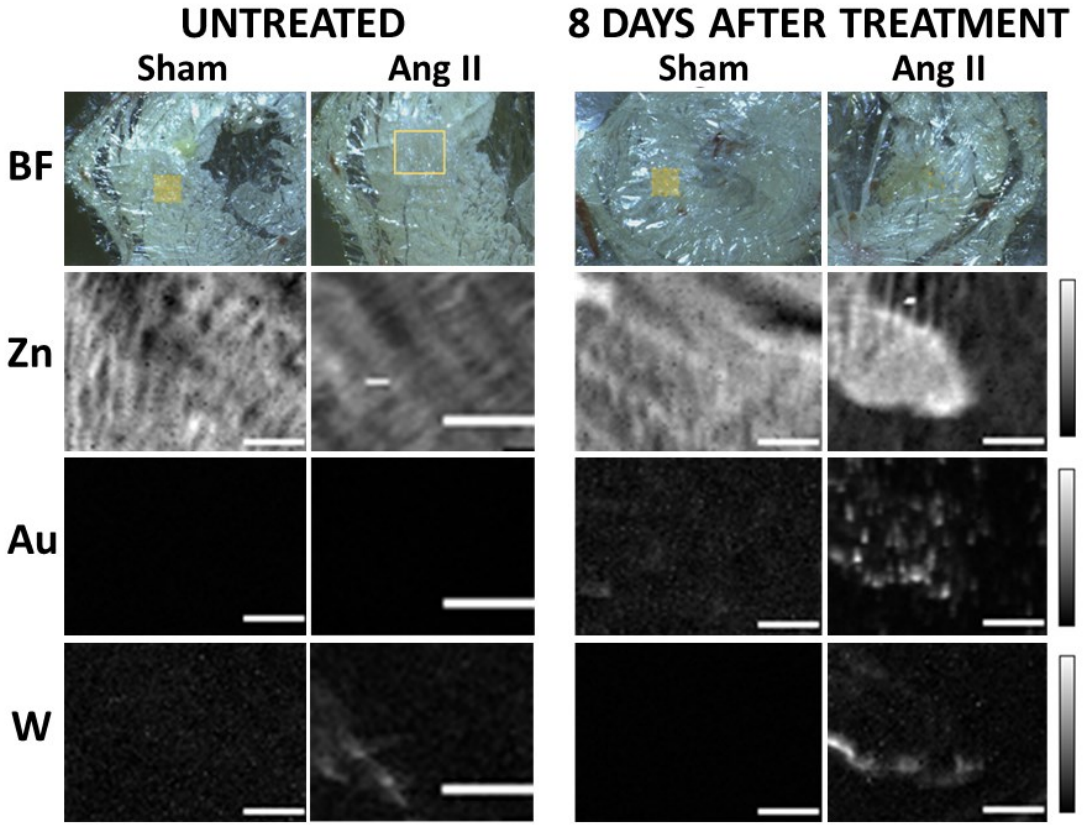

Figure S24. Heart sections from healthy (Sham) or fibrotic (Ang II) mice, untreated (vehicle treated) or8 days after **4-AuNC** treatment, showing the areas studied with SXRF. Bright field (BF) and Zn, K, Au, and W SXRF elemental maps showing localization of Zn, Au, or W elements in those areas; Raster scan: 5x5 μm^2 step size, 1 s dwell time. Scale bar 100 µm. Concentration range in images: 0-4 ng mm^{-2} Zn, 0-2 ng mm^{-2} Au, or 0-3 ng mm^{-2} W.

Gene expression of Hsp90

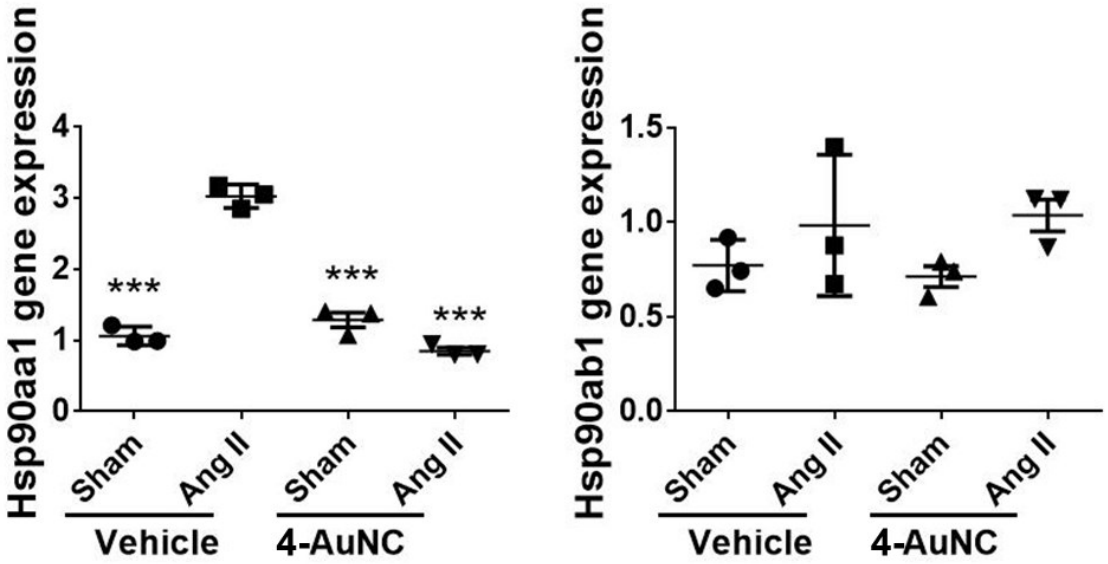

Figure S25. Gene expression of Hsp90aa1 and Hsp90ab1 in the heart of healthy (Sham) and Fibrotic (Ang II) controls (Veh) and healthy (Sham) and Fibrotic (Ang II) **4-AuNC** treated mice. Data were expressed as mean ±SD in arbitrary units (***$p<0.001$; Mann-Whitney test).

References

1. E. R. Main, Y. Xiong, M. J. Cocco, L. D'Andrea and L. Regan, *Structure*, 2003, **11**, 497-508.
2. T. Kajander, A. L. Cortajarena, E. R. Main, S. G. Mochrie and L. Regan, *J Am Chem Soc*, 2005, **127**, 10188-10190.
3. A. L. Cortajarena, F. Yi and L. Regan, *ACS Chemical Biology*, 2008, **3**, 161-166.
4. A. L. Cortajarena, S. G. Mochrie and L. Regan, *Protein Sci.*, 2011, **20**, 1042-1047.
5. A. Aires, I. Llarena, M. Moller, J. Castro-Smirnov, J. Cabanillas-Gonzalez and A. L. Cortajarena, *Angewandte Chemie International Edition*, 2019, **58**, 6214-6219.
6. T. Z. Grove, M. Hands and L. Regan, *Protein Engineering Design and Selection*, 2010, **23**, 449-455.
7. A. L. Cortajarena and L. Regan, *Protein Science*, 2006, **15**, 1193-1198.
8. R. Eachkoti, M. V. Reddy, Y. K. Lieu, S. C. Cosenza and E. P. Reddy, *Eur J Cancer*, 2014, **50**, 1982-1992.
9. V. A. Solé, E. Papillon, M. Cotte, P. Walter and J. Susini, *Spectrochimica Acta Part B: Atomic Spectroscopy*, 2007, **62**, 63-68.
10. J. Schindelin, I. Arganda-Carreras, E. Frise, V. Kaynig, M. Longair, T. Pietzsch, S. Preibisch, C. Rueden, S. Saalfeld, B. Schmid, J.-Y. Tinevez, D. J. White, V. Hartenstein, K. Eliceiri, P. Tomancak and A. Cardona, *Nature Methods*, 2012, **9**, 676-682.

11. T. Kajander, A. L. Cortajarena, E. R. G. Main, S. G. J. Mochrie and L. Regan, *Journal of the American Chemical Society*, 2005, **127**, 10188-10190.
12. T. Kajander, A. L. Cortajarena, S. Mochrie and L. Regan, *Acta Crystallographica Section D Biological Crystallography*, 2007, **63**, 800-811.
13. C. C. Huang, Z. Yang, K. H. Lee and H. T. Chang, *Angewandte Chemie*, 2007, **46**, 6824-6828.
14. M. A. Muhammed, P. K. Verma, S. K. Pal, R. C. Kumar, S. Paul, R. V. Omkumar and T. Pradeep, *Chemistry*, 2009, **15**, 10110-10120.
15. A. M. Hussain, S. N. Sarangi, J. A. Kesarwani and S. N. Sahu, *Biosensors & bioelectronics*, 2011, **29**, 60-65.
16. L. Yang, J. Chen, T. Huang, L. Huang, Z. Sun, Y. Jiang, T. Yao and S. Wei, *Journal of Materials Chemistry C*, 2017, **5**, 4448-4454.
17. H. Kawasaki, K. Hamaguchi, I. Osaka and R. Arakawa, *Advanced Functional Materials*, 2011, **21**, 3508-3515.
18. H. Ding, H. Li, X. Wang, Y. Zhou, Z. Li, J. K. Hiltunen, J. Shen and Z. Chen, *Chemistry of Materials*, 2017, **29**, 8440-8448.
19. C. Wang, L. Ling, Y. Yao and Q. Song, *Nano Research*, 2015, **8**, 1975-1986.
20. X. Jia, J. Li and E. Wang, *Small*, 2013, **9**, 3873-3879.
21. R. Garcia, D. Merino, J. M. Gomez, J. F. Nistal, M. A. Hurle, A. L. Cortajarena and A. V. Villar, *Cell Signal*, 2016, **28**, 1563-1579.
22. R. A. Cáceres, T. Chavez, D. Maestro, A. R. Palanca, P. Bolado, F. Madrazo, A. Aires, A. L. Cortajarena and A. V. Villar, *Journal of Molecular and Cellular Cardiology*, 2018, **123**, 75-87.
23. W. J. Li, Y. Liu, J. J. Wang, Y. L. Zhang, S. Lai, Y. L. Xia, H. X. Wang and H. H. Li, *Life Sci*, 2016, **149**, 18-24.
24. Q. Wang, Y. Yu, P. Zhang, Y. Chen, C. Li, J. Chen, Y. Wang and Y. Li, *Basic Res Cardiol*, 2017, **112**, 017-0634.